Energy Advances

PAPER

View Article Online
View Journal | View Issue

Cite this: *Energy Adv.*, 2022, 1, 1009

Brute force determination of the optimum pore sizes for CO_2 uptake in turbostratic carbons†

L. Scott Blankenship, *[a] Nawaf Albeladi, ‡[ab] Thria Alkhaldi, ‡[ac] Asma Madkhali ‡[ad] and Robert Mokaya [a]

Porosity, and in particular pore size is one of the most important considerations in the development of porous carbons for CO_2 capture. Current methods for determining the optimum pore size for adsorption of gases either make very broad assumptions (in computational studies), or are not sufficiently exhaustive (in experimental studies). Herein we present a piece of software known as the python Porosity Uptake Correlator (pyPUC) which employs a brute force, first principles method for determining the range of pore sizes, Ω, best suited to adsorption of a given sorptive at a range of pressures. As an initial test, pyPUC is used to determine Ω for CO_2 in a broad pressure range according to N_2 porosimetry. The analysis is then extended to other porosimetric sorptives and combinations thereof to assess their efficacy in determining Ω for CO_2, and we find that traditional N_2 porosimetry is insufficient for determining the relationship between pore size and CO_2 uptake in ultramicroporous turbostratic carbons. While pyPUC is not meant as a predictive tool, it facilitates a more robust and thorough investigation of the relationship between porosity and adsorbate uptake capacity than current methods, and provides a method for understanding such relationships more generally.

Received 21st June 2022,
Accepted 24th October 2022

DOI: 10.1039/d2ya00149g

rsc.li/energy-advances

1 Introduction

Porous carbons have been extensively investigated for their potential use in gas storage and/or capture applications, in particular related to energy storage applications including for alternative fuels such as H_2 and CH_4 or for CO_2 capture.[1–9] A material's storage capacity for a particular sorptive is known to be related to the porosity of the material, and in particular the pore width plays an important role.[5,10–21] Pore entrances for sorption of some gas at a given pressure and temperature must be large enough for the molecule in question can diffuse into it. This lower limit to the so-called pore size range is not necessarily solely determined by the size of the molecule; for example while N_2 has a nominal kinetic diameter (d_k) of 3.60 Å, it has been observed that at −196 °C in biochars this molecule diffuses extremely slowly into pores of width 4 Å.[22–24] On the other hand, adsorption can be improved by optimising the interactions between parallel pore walls and adsorptive molecules. That is, when the distance between pore walls is sufficiently small, adsorbed molecules are affected by physical attraction to both walls, which increases the heat of adsorption and thus the retention of molecules within the pores.[25,26] This is particularly significant at low pressures where the adsorbate–adsorbent interactions dominate.[13,15,27–34] It follows therefore, that there is a range of optimum pore sizes for adsorption of any given molecule at some pressure and temperature.

There have been several attempts to determine the optimum pore size for given sorptives under some conditions. In general, the approach to this has been to either identify the 'ideal' pore size, *i.e.* a single width such as 6 Å for H_2 with slight variations depending on temperature and pressure.[12,28] An alternative method is to propose larger regions, *i.e.* an optimum pore size range (herein referred to as Ω);[15,35,36] for H_2 it has been reported that ultramicropores, *i.e.* pores of width <7 Å are ideal.[20,31] Sdanghi *et al.* expanded on this, finding that pores narrower than 6.0 Å are essential for maximising H_2 storage at pressures below 1 bar, while broader PSDs are more relevant at higher pressures.[37] In practice, these regions or single widths are determined *via* purely computational methods or from experimentally determined uptakes and pore size distributions (PSDs). Computational methods attempt to determine the uptake of the sorptive in an idealised sorbent with pores of a

[a] School of Chemistry, University of Nottingham, University Park, Nottingham, NG7 2RD, UK. E-mail: leo.blankenship@nottingham.ac.uk
[b] Chemistry Department, Faculty of Sciences Yanbu, Taibah University, Yanbu Al Bahr, 46423, Saudi Arabia
[c] Department of Chemistry, Jeddah University, Jeddah 23442, Saudi Arabia
[d] Department of Chemistry, University College in Samtah, Jazan University, Samtah 86736, Saudi Arabia

† Electronic supplementary information (ESI) available: Supplementary figures and tables; raw (.aif) isotherms; PSD and modelling analysis summaries as.csv; and raw outputs of D_v, D_π, and D_c for each DataSet (.csv) available at https://github.com/sblanky/pyPUC_si; source code available on https://github.com/sblanky/pyPUC. See DOI: https://doi.org/10.1039/d2ya00149g

‡ These authors contributed equally to this work.

single width *via* Density Functional Theory (DFT) or Grand Canonical Monte Carlo (GCMC) methods.[5,12,38] Whereas experimental data can be used to performing linear regressions of uptake at a given pressure against pore volume in a certain range (usually all pores below some maximum).[11,13,15,17,35,39] By the latter method, Presser *et al.* determined (N = 24) that at 1.0 bar, pores in activated carbons of width <8 Å are most strongly associated with gravimetric CO_2 uptake, while this reduced to 5 Å for uptake at 0.1 bar. Pores larger than 10 Å, as well as the oft-used parameter of average pore size were shown to be poor predictors of uptake at these low pressures.[13] Average pore size can however be useful when compared against so-called uptake density (uptake per unit surface area). For example, Masika *et al.* found that uptake density of H_2 (1 bar, −196 °C) reduced drastically as average pore width increased from 10 to 20 Å.[16]

Current experimental approaches to determining Ω are limited in that they typically only consider a small set of possible Ωs, which is informed by theoretical data, and only at one or two pressures. Furthermore, the lower limit of the Ω is not typically varied – the assumption being that pores larger than the diameter of the sorptive will always be strong contributors to sorptive uptake under all conditions. As for computational studies, not only is the use of materials having a single pore width unrealistic for amorphous porous carbon, it is difficult to account for factors such as surface chemical and energetic heterogeneity and variation in pore geometry. Thus we present herein the python Porosity Uptake Correlator (pyPUC); a combined, iterative experimental and computational approach to Ω determination. Regressions are performed using experimental data between all possible Ωs at a large range of pressures and used to determine the Ω at each pressure. Both the range and increment of the possible Ωs and pressures can be easily adjusted to give an extremely fine level of detail. As a demonstration, pyPUC is applied to the determination of Ω for CO_2 uptake in amorphous carbons at 25 °C where porosity is determined from N_2 sorption isotherms obtained at −196 °C. The relative efficacy of H_2, O_2, and N_2 (−196 °C) isothermal porosimetry as well as dual fit N_2/H_2 and O_2/H_2 analyses is then assessed for their ability to predict Ω for CO_2 in highly ultramicroporous carbons.

2 Methods

2.1 pyPUC

The pyPUC software requires both total gravimetric uptake isotherms (υ) for the adsorptive in question, and cumulative PSDs (π) for a set of porous samples. Firstly, a model isotherm is fit to each experimental isotherm in υ using the pyGAPS adsorption isotherm processing framework, *via* the modelling package initially developed in pyIAST.[40,41] These model isotherms are converted to point isotherms according to some user-defined pressure range and increment. Thus, discrete loadings are determined for all samples at identical pressures, and are stored in the loading DataFrame (D_υ).

Next, from π the apparent pore volume (V) or surface area (S) of each sample between the minimum and maximum pore width (w_{min} and w_{max}, respectively) is determined *via*;

$$\begin{aligned} V &= V(w_{max}) - V(w_{min}), \\ S &= S(w_{max}) - S(w_{min}) \end{aligned} \quad (1)$$

This is repeated across all pairs of w_{max} and w_{min} prescribed by the user, thus generating a parameter DataFrame (D_π). The number of parameters calculated N_π is thus related to the number of pore widths defined in the calculation N_w by;

$$N_\pi = \frac{1}{2}\frac{N_w!}{(N_w-2)!} \quad (2)$$

Thereafter, linear regressions are determined between every row of D_υ and D_π to give the correlation DataFrame (D_c), *i.e.* D_c shows how well porosity (in terms of V or S) within each pore width range in D_π correlates to the loading of the sorptive on the samples at each pressure in D_υ. Each row of D_c contains the Pearson coefficient (r^2),[42] slope (m) and intercept (c) of the regression. Finally, the best correlation at each pressure may be found simply by selecting the maximum r^2 value for a given pressure after the exclusion of regressions giving a negative slope. This is repeated for all pressures, giving the Ω associated with uptake of the sorptive at each pressure.

2.2 Carbon synthesis

Carbons were synthesised by pyrolysis of various biomasses and synthetic polymers either alone or with the aid of a porogen. In all cases they were washed after synthesis to remove any non-carbonaceous matter. Synthetic summaries are provided in for DataSet 1 (33 samples) and DataSet 2 (12 samples) in Tables S1.1 and S2.1 (ESI†) respectively. DataSet 1 was selected to give a large variety of PSDs that are representative of so-called activated carbons in general; that is samples in this group have either solely microporous, solely mesoporous or hierarchical (*i.e.* mixed) PSDs. DataSet 2 contains principally microporous materials, especially those containing a large proportion of so-called ultramicropores (w < 7).

2.3 Isotherm measurement and processing

All raw experimental isotherms measured as described below are available in the electronic ESI,† as human- and machine-readable .aif files.[43] N_2, O_2, and H_2 isotherms for determination of PSDs were measured at −196 °C on a Micromeritics 3flex porosimeter at pressures up to P_0 for N_2 and O_2 and 1013 mbar for H_2. PSDs were determined using the SAIEUS software with the appropriate 2D-NLDFT heterogeneous surface kernel(s), in order to adequately account for chemical and energetic heterogeneity. Within SAIEUS it is possible to select an appropriate fitting parameter, λ[44–46] which controls the roughness of the PSD. λ was selected to provide the most realistic differential PSD based on known properties of carbons, and in all cases was between 2.5 and 5.0 and kept constant for carbons derived from the same precursor (see Tables S1.1 and S2.1, ESI†). Isotherms

and derived PSDs can be found in Fig. S1.6–S1.10 and S2.4–S2.12 (ESI†).

Gravimetric CO_2 uptakes were measured on gravimetric analysers provided by Hiden; either the XEMIS analyser at 25 °C (0–40 bar) or the IGA at 18 °C (0–20 bar) for DataSet 1 and 2 respectively. Fits were attempted with Langmuir,[47,48] Double Site Langmuir (DSLangmuir),[48] Triple Site Langmuir (TSLangmuir),[48] Guggenheim–Anderson–de Boer (GAB),[49–51] Freundlich,[52] Dubinin–Raduschkevich (DR)[53] and Toth[54] theoretical isotherms using pyGAPS (see Section 2.1). The best fit was then selected by minimum root mean square error (RMSE). CO_2 isotherms as well as their best fits and details thereof can be found in Fig. S1.1–S1.5 and S2.1–S2.3 (ESI†).

3 Results and discussion

3.1 From N_2 isotherms only

We first present the use of pyPUC to determine Ω according to porosity derived from isotherms of the ''traditional'' porosimetric molecule, N_2. This is to establish the validity of this brute force method and to compare results derived in this way to those reported in the literature. A set of 33 carbon samples were used in this section.

3.1.1 DataFrame preparation. The 33 activated carbons and biochars used in the initial analysis have varied PSDs in the range 3.6–100 Å (by pore volume) according to fits to N_2 isotherms with the 2D-NLDFT heterogeneous surface kernel (see Fig. S1.6–S1.10, ESI†). It was possible to fit model isotherms to the experimental CO_2 isotherms in the full range 0.10–40 bar with a maximum root mean square error (RMSE) of 0.168 (Fig. S1.1–S1.5, ESI†), although fits were slightly poorer for some isotherms at low pressures, notably *aP-2800*, *aP-2900* and *aP-3700* (Fig. S1.1(b2, b3, b5), respectively, ESI†). It should be noted, that while a wide range of model fits were attempted, only DSLangmuir, TSLangmuir and Toth models provided the best fits to the experimental isotherms. DSLangmuir was by far the most common best fit, while Toth was only used for two samples. The model isotherms were output as 40 points in the range 0.1–40 bar defined using a base-10 logarithmic increment between points to give D_υ. Similarly, D_π was calculated using a base-10 logarithmic increment to give 100 w values between 3.6 and 100 Å. Determination of D_c therefore required 198 000 linear regressions, which were used to determine the Ω at each of the 40 pressures defined in D_υ in terms of V and S *i.e.* Ω_V and Ω_S respectively. A more detailed calculation, using a D_π of 500 values between 3.6 and 500 Å was also performed in order to ascertain the effect of increasing the granularity of detail used in the input data on the calculated Ω. This calculation took almost 7 days each for Ω_V and Ω_S compared to the original calculation which was completed within 24 h and results are not significantly different. As such this data was not used as the basis of the study. A comparison can be seen in Fig. S1.11 (ESI†).

3.1.2 The optimum pore size region, Ω. Fig. 1 shows Ω_V (a) and Ω_S (b) in the pressure range studied. As expected, in both cases the range of Ω broadens with increasing pressure. This shows the positive effect to high pressure CO_2 uptake of more hierarchical PSDs. It is also notable that in the case of both V and S while w_{max} increases almost constantly, there are basically only two values for w_{min}, starting at 3.6 Å and then increasing to around 7.0 Å at some pressure. In other words, there is a pressure range in which ultramicropores are strongly associated with CO_2 uptake. This range is up to 7.4 and 3.4 bar for V and S, respectively.§ At 0.10 bar, w_{max} is approximately 8 Å and increases to 17 and 11 Å for V and S, respectively once Ω begins to exclude the ultramicropores. That is, with increasing pressure supermicropores have an increasing influence on CO_2 uptake. The fact that the pressure range wherein w_{min} is 3.6 Å is much smaller for S relative to V may be a result of reduced influence of London interactions between the carbon surface and the sorptive as pressure increases. Increased pressure means that multilayer adsorption, and thus interactions between CO_2 molecules becomes more dominant.

Once Ω begins to exclude ultramicropores, there is a sharp increase in w_{max}. As a result, Ω_S includes both supermicropores and small mesopores after 6 bar. Conversely, Ω_V remains strictly in the supermicropore region until 13 bar. Again, this seems to be an indication of the difference in the how surface area *vs.* pore volume improve adsorption of CO_2. That is smaller pores result in improved sorptive–sorptive interactions, while larger pores provide more surface for CO_2 to interact with. This is further exhibited by the large increase in w_{max} up to 100 Å for Ω_S at 16 bar which does not exist for Ω_V. Of course, this upper limit for Ω_S is not real but represents the upper limit of w_{max} established in the determination of D_π. Nevertheless, these results may inform design of porous carbons for different applications; for example a carbon with high porosity below 8.0 Å is best suited for low pressure capture of CO_2, whereas carbons for so-called pressure-swing adsorption (PSA) should have hierarchical micro-mesoporous PSDs with minimal porosity below 8.0 Å. This confirms previous reports.[13,15,27,55,56]

3.1.3 Relative strength of correlations. Fig. 1, however does not tell the full story as it presents each of the Ωs as equal. That is, there is no consideration of relative Pearson coefficients (r^2), which is presented in Fig. 2. While positive correlations were established for each pressure in question, r^2 ranges from 0.57 at 0.10 bar (Fig. 2(a1)) to 0.88 at 40 bar (Fig. 2(d1)). Indeed, r^2 steadily improves with increasing pressure and this trend is shared both for the volume and surface area of pores within Ω, *i.e.* V_Ω and S_Ω respectively. The relatively poor fit at low pressure may be a result of the imprecision of PSDs derived from N_2 isotherms in the ultramicropore region.[22,24,34] In addition, as mentioned before fitting of models to CO_2 isotherms to $P < 1.0$ bar was in some cases less successful than for higher pressures, thus there may be inaccuracies in the determined gravimetric uptake at such pressures.

3.1.4 Effect of increasing pressure on influence of Ω on CO_2 uptake. Fig. 2 also shows the approximate relationship

§ In the more detailed calculation (see Fig. S1.11, ESI†) this limit is found to be slightly lower.

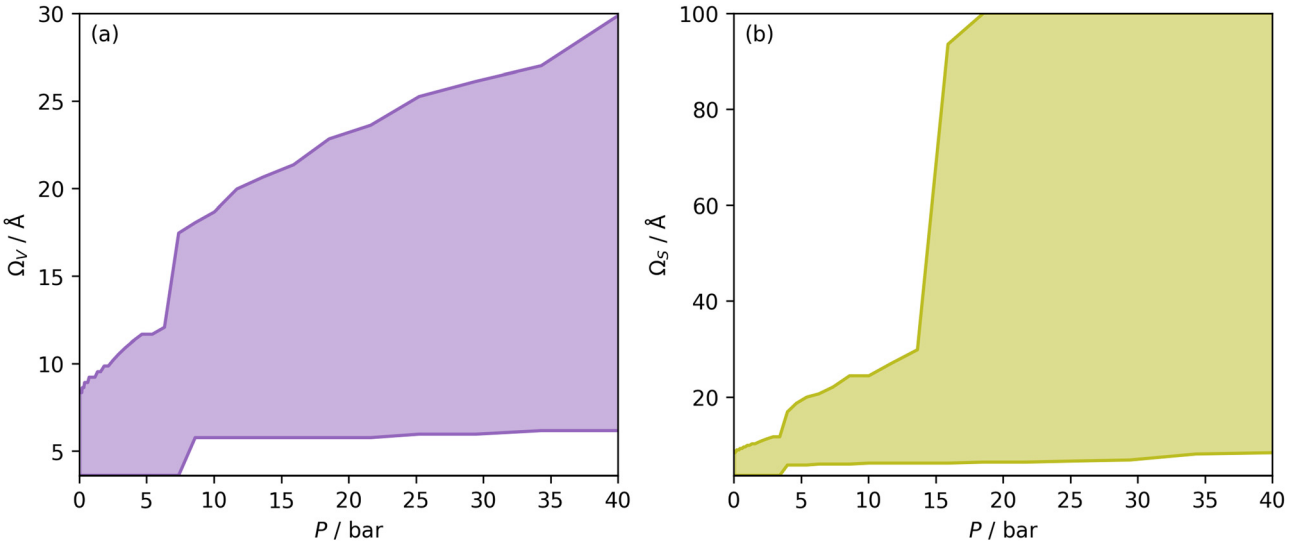

Fig. 1 Ω_V (a) and Ω_S (b) at each pressure, *i.e.* optimum w_{max} and w_{min} plotted against pressure. The shaded area is thus the Ω in each case.

between uptake at the pressure (U) in question and pore volume or surface area within the Ω in the form $\frac{dU}{dV_\Omega}$ or $\frac{dU}{dS_\Omega}$, as derived from the linear regression. It is thus possible to predict the effect of increasing pore volume within the Ω on CO_2 uptake at that pressure, *i.e.* increasing volume of pores of width 3.6–8.3 Å by 1 $cm^3\ g^{-1}$ ought to result in an increase in uptake of 1.7 mmol g^{-1} CO_2 at 0.1 bar, whereas the same increase in pore volume in the range 6.2–30 Å (approximately the supermicropore and small mesopore region) results in an improvements in CO_2 uptake at 40 bar of 18 mmol g^{-1}. If we examine slopes of fits in Fig. 2, (column b), a similar pattern appears, with an increase in surface area of 1000 $m^2\ g^{-1}$ in pores between 3.6 and 8.3 Å corresponding to a meager 0.57 mmol g^{-1} improvement in CO_2 uptake at 0.1 bar compared with an increase in uptake of 11 mmol g^{-1} at 40 bar when surface area in pores of width 8.3–100 Å increases by the same amount.

Furthermore, a clear positive, semi-logarithmic trend is observed between $\frac{dU}{dV_\Omega}$ and P, *i.e.* it takes the form of a gas adsorption isotherm (see Fig. 3). A similar transform to that used in determination of a Langmuir isotherm[47] demonstrates a strong relationship of the form;

$$\frac{dU}{dV_\Omega} = \frac{P}{mP + c} \quad (3)$$

where the slope m is 0.054 $cm^3\ mmol^{-1}$ with an r^2 of 0.997. The intercept, c does not have any physical significance as it ought to be a product of CO_2 uptake at 0 bar, and thus should be zero. Its non-zero value is likely a reflection of the relatively high uncertainty in the relationship between U and V at pressures below 1 bar. A similarly strong fit (r^2 = 0.980) can be observed for $\frac{dU}{dS_\Omega}$ by the same treatment as in eqn (3), where m = 93 $m^2\ mmol^{-1}$. However the relationship between $\frac{dU}{dS_\Omega}P$ and P is not exactly linear. Nevertheless, it is clear that with increasing pressure, improvements in Ω_V or Ω_S correspond to rapid improvements in U at low pressures, but these improvements diminish at higher pressures. This is likely a result of a reduction in enthalpy of adsorption with increasing adsorbate loading.

3.1.5 Association of arbitrary pore-size regions with uptake. While Sections 3.1.2, 3.1.3, and 3.1.4 discuss Ω, *i.e.* the absolute best pore size range for CO_2 uptake at a given pressure (according to the described methods), experimentally targeting porosity of amorphous porous carbons within such precise limits (*e.g.* 3.6–9.2 Å at 1 bar) is unlikely to be practicable. Besides, these limits are 'fuzzy', in that the 'next best pore' size region to Ω typically has a similar r^2 value at the pressure in question. It is useful therefore to examine the dependence of r^2 as determined in the D_c on pressure within specific pore size regions, as shown in Fig. 4. For brevity, these results are discussed and displayed in terms of pore volume only. The traditional division of nanopores separates micropores into so-called ultramicropores (<7 Å) and supermicropores (7–20 Å). As shown in Fig. 4(a1) ultramicropores are not particularly strongly associated with CO_2 uptake at any pressure, although r^2 does improve at low pressures – in contrast to previous reports.[13,15] On the other hand, supermicroporosity does appear to correlate fairly strongly ($0.6 < r^2 < 0.8$) with uptake at pressures between 10 and 40 bar. This analysis also shows that mesoporosity does not show any particularly strong relationship with a carbon's ability to capture CO_2 at any pressure below 40 bar – the maximum r^2 is only 0.52. That is not to say that mesopores are not important for high pressure CO_2 adsorption, indeed as discussed in 3.1.2, both Ω_V and Ω_S at 40 bar include small mesopores, in addition to supermicropores, with r^2 of 0.88 and 0.84, respectively.

In Section 3.1.2 and Fig. 1 we see that at lower pressures Ω is approximately 3.6–10 Å. Therefore, a reasonable alternative to the traditional subdivision of micropores at 7 Å could be at 10 Å.

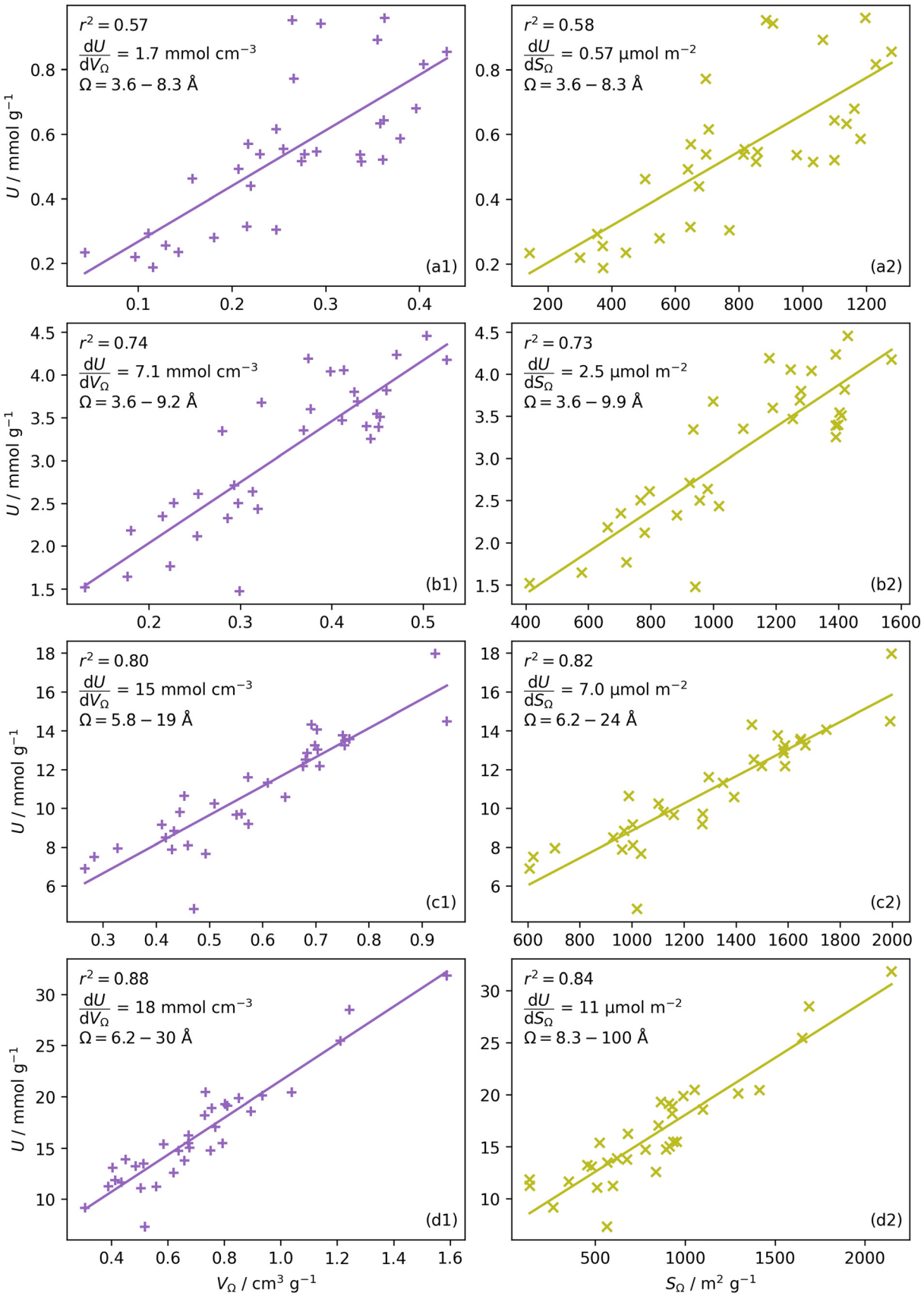

Fig. 2 CO_2 uptake, U *vs.* pore volume, V_Ω (column a) and surface area, S_Ω column (b) in Ω, at 0.10 (row 1), 1.0 (row 2), 10 (row 3), and 40 (row 4) bar.

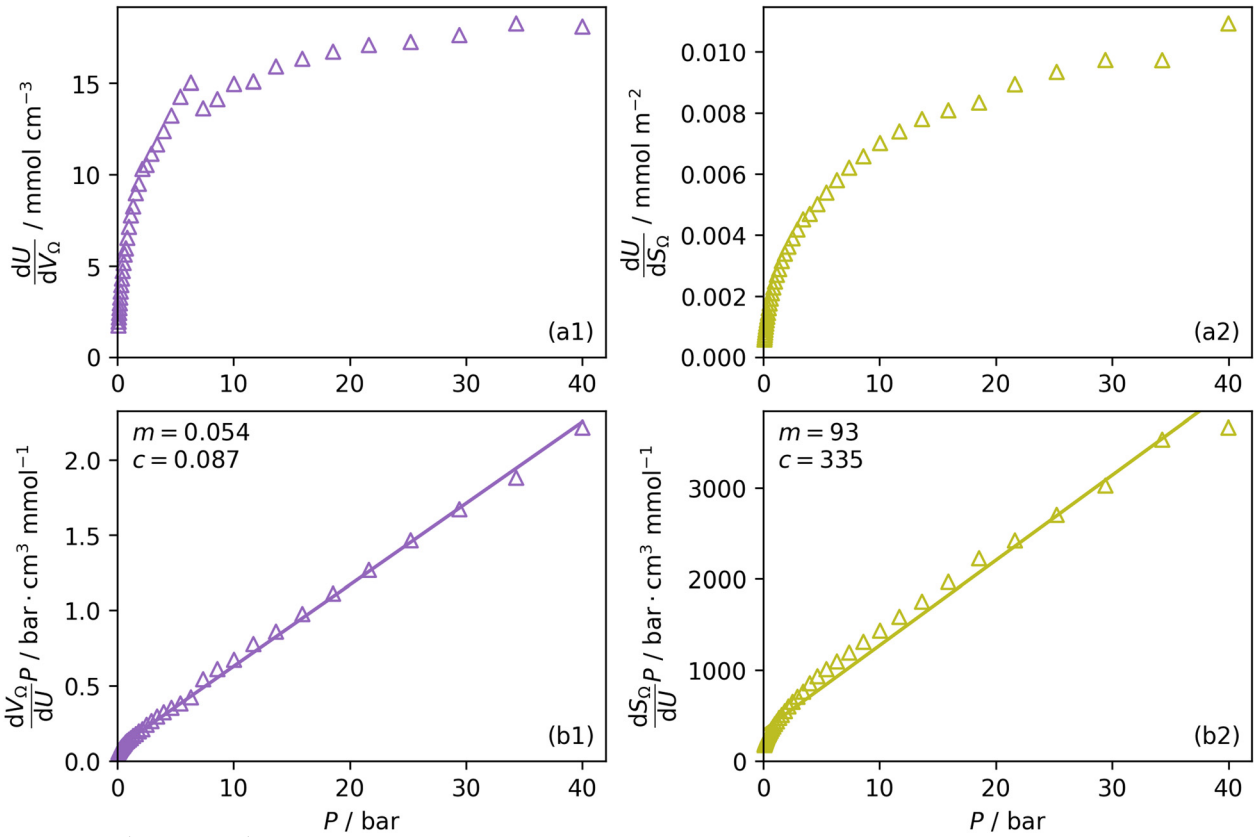

Fig. 3 Change in $\frac{dU}{dV_\Omega}$ (a1) and $\frac{dU}{dS_\Omega}$ (a2) with P, and in a linearised form (b1) and (b2).

As shown in Fig. 4(a2), pores of width <10 Å do indeed show improved correlation with CO_2 uptake at relatively low pressures with r^2 reaching 0.79 at 2.9 bar. Conversely the larger subdivision, *i.e.* between 10 and 20 Å does not show improvements relative to the supermicropore designation, and has much poorer correlations at high pressures. Expanding this pore size region to include all pores above 10 Å does not significantly improve r^2 values in the pressure range used in this study. In other words it appears that pore size regions to target for high (10–40 bar) and medium (<10 bar) pressure uptake overlap, with the former being pores above 7 Å, and the latter below 10 Å. Low pressures (<1 bar) require even smaller pores of widths less than 8–9 Å (see Fig. 1 and 2(a1-2, b1-2)).

Fig. 4(b1 and b2) show the effect of a broadening pore size region on the relationship between r^2 and P, with a fixed lower limit of 3.6 and 7.0 Å respectively. These lower limits correspond to the two values of w_{min} mentioned in 3.1.2. In both cases small increases in w_{max} have a strong affect on the pressure at which correlation is strongest for the pore size region. However at higher values of w_{max}, this discrepancy is reduced. For example pores of width 7.0–31 and 7.0–90 Å have their strongest association ($r^2 \approx 0.85$) with CO_2 uptake at 40 bar. This corresponds roughly to Ω_V at 40 bar (Fig. 2(d1)) and shows that at high pressures larger pores may not significantly effect adsorption of CO_2. It is interesting to note that very narrow pore size ranges *i.e.* 3.6–4.7 and 3.6–6.2 Å (Fig. 4(b1)) do not show any significant relationship to CO_2 uptake, in fact r^2 never exceeds 0.27 for either of these pore size regions, so any variation in r^2 here is of limited interpretation. That is, there appears to be a lower limit to pore size that positively affects uptake at pressures of 0.10 bar and greater which is around 8.1 Å.

3.2 Highly ultramicroporous carbons

We recently reported on relative improvements in the precision of PSDs determination by use of dual fits of DFT kernels to O_2 and H_2 isotherms relative to using N_2 and H_2.[34] This was particularly relevant to so-called biochars and carbons activated with small amounts of porogen, both having a high proportion of ultramicropores. The rationale being that N_2's poor diffusion into ultramicropores meant that PSDs, especially at the smaller end of the micropore region, are imprecise. In addition, when NLDFT kernels were fit to N_2, O_2 and H_2 isotherms individually there were notable discrepancies in derived PSDs, which were more evident for the more ultramicroporous carbons.[34] In the previous section it was noted that the Pearson coefficient for Ω was very low at low pressures, which may be a result of imprecise PSDs for DataSet 1 in the ultramicropore region. It is useful therefore to examine the relative results of Ω determination using PSDs from single N_2, O_2 and H_2 isotherms as well as from dual kernel fitting. The following sections examine PSDs from these sorptives and combinations thereof in the determination of optimum porosity in the 12 carbons in

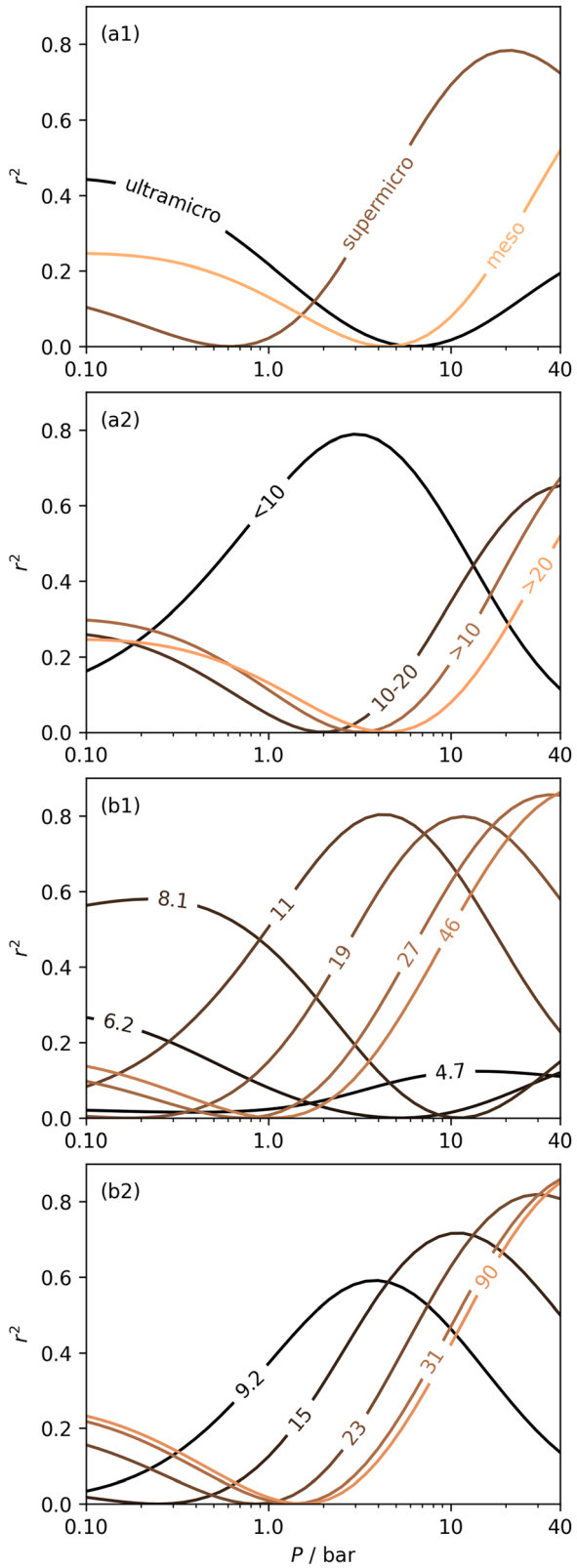

Fig. 4 Dependence of r^2 on pressure within different pore size regions by pore volume, *i.e.* ultramicropores, supermicropores and mesopores (a1); pores of width <10, 10–20, >10, and >20 Å (a2); increasing w_{max} with a fixed w_{min} of 3.6 (b1) and 7.0 Å (b2).

DataSet 2. Synthetic details for these samples can be found in Table S2.1 (ESI†).

3.2.1 Analysis using PSDs from single isotherm H_2, N_2, and O_2 fits. CO_2 uptake isotherms, their fits, and PSDs from the three sorptives can be found in Fig. S2.1–S2.3 and S2.4–S2.6 (ESI†). A comparison of Ω_V derived using each of the three isotherms (*i.e.* $\Omega_V^{\text{sorptive}}$) in question in the pressure range 0.10–20 bar can be found in Fig. 5.¶ It is clear that no single sorptive is providing a reasonable Ω_V for DataSet 2 throughout the prescribed pressure range. In particular, Ω_V from N_2 $\left(\Omega_V^{N_2}\right)$ isotherms (Fig. 5(a1)) gives the unreasonable conclusion that up to 2.1 bar $\Omega_V^{N_2}$ is constant at around 5.8–6.3 Å. This is both a surprisingly narrow range, and it is unlikely that there would be effectively no broadening of $\Omega_V^{N_2}$ with increasing P up to this point. Similarly, after 2.1 bar $\Omega_V^{O_2}$ (Fig. 5(a2)) drops to a very narrow, relatively constant range (approximately 10–11 Å). This may simply be an effect of the minimal increases in CO_2 uptake for these carbons above 2 bar (see Fig. S2.1–S2.3, ESI†), which is attributable to the very low porosity of these carbons in the supermicropore and mesopore regions (see Fig. S2.4–S2.6, ESI†).[34] As such discussions of these analyses are best limited to uptakes at $P < 2.0$ bar.

For analyses using both O_2 and H_2 there is a broadening in Ω_V with increasing P at relatively low pressures which is not present according to N_2 analysis. In addition, as shown in Fig. 5(b), r^2 is lower at all pressures for correlations derived using $\Omega_V^{N_2}$ data compared to $\Omega_V^{O_2}$ and $\Omega_V^{H_2}$. While $\Omega_V^{O_2}$ data shows the best correlations in general, r^2 from $\Omega_V^{H_2}$ data is greater at 0.10 and 0.13 bar. In other words, for this set of carbons, porosity accessible to CO_2 is best determined using H_2 isotherms up to 0.13 bar, and thereafter (up to around 2.0 bar) using O_2 isotherms. This follows from the standpoint of H_2 having access to – and thus predicting the presence of – pores of widths as small as 3.0 Å, while the lower limit for O_2 is 3.6 Å. Thus the contribution of pores of widths less than 3.6 Å to low pressure CO_2 uptake can only be accounted for using H_2 porosimetry, yielding $\Omega_V^{H_2} = 3.3 - 5.9$ Å. At 0.17 bar and above, pores above 6.0 Å appear to become more heavily utilised for CO_2 adsorption according to relative magnitudes of r^2. The upper limit of porosity measurable by H_2 at −196 °C is unknown, however it is usually said to be between 8.0–10 Å.[22,24] This explains why results for $\Omega_V^{H_2} = 3.3 - 5.9$ Å become less reasonable at pressures above 0.3 bar; H_2 porosimetry is unsuitable for prediction of CO_2 uptake at these pressures. Indeed, in determination of PSDs from fitting of the DFT kernel to H_2 isotherms, w_{max} was set to 10 Å.

Fig. 6 presents further information on the relative efficacy of the three sorptives in measuring pores of widths below some limit (w_{max}), and the relationship between pores of these widths and CO_2 uptake between 0.10 and 2.0 bar. It is striking that when w_{max} is set at 5.0 or 6.0 Å, only H_2 porosimetry provides

¶ Results for $\Omega_S^{\text{sorptive}}$ are sufficiently similar to not require a separate discussion here. A comparison is displayed in Fig. S2.13 (ESI†).

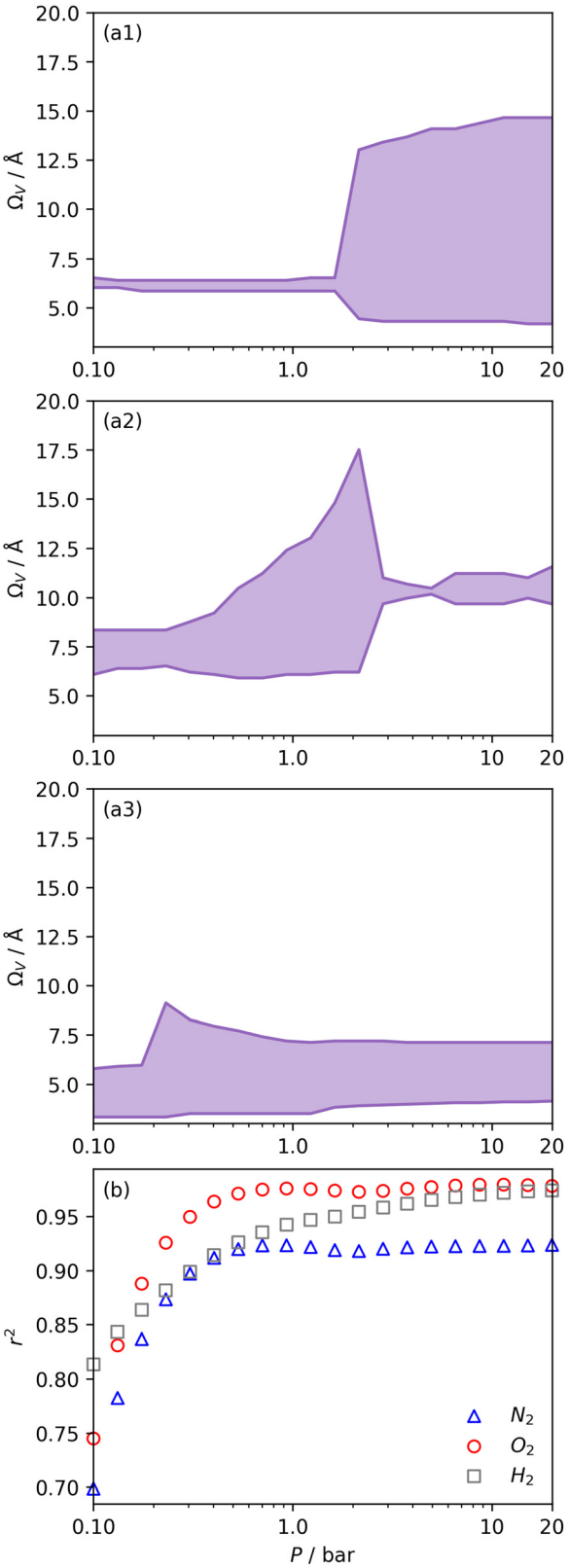

Fig. 5 Ω_V calculated from DataSet 2 using PSDs derived from N_2 (a1), O_2 (a2), and H_2 (a3) isotherms as well as corresponding r^2 values (b).

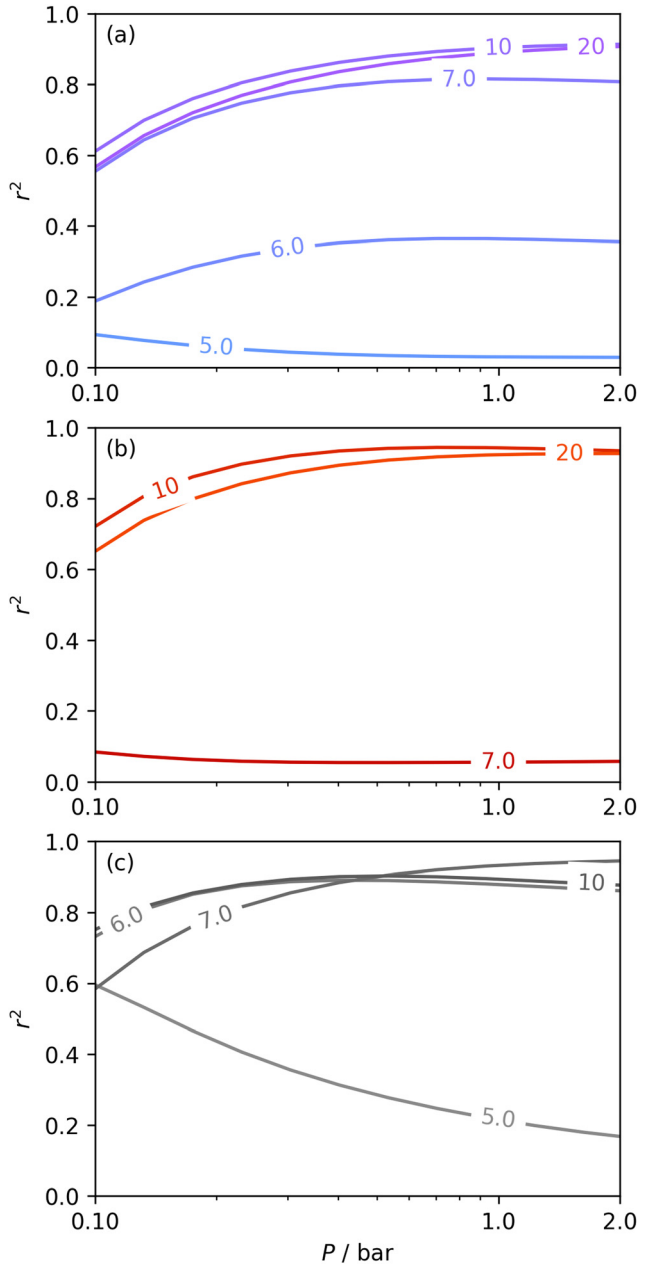

Fig. 6 Comparison of dependence of r^2 on pressure with increasing w_{max} as determined using PSDs from N_2 (a), O_2 (b), and H_2 (c) isotherms.

reasonable correlations ($r^2 > 0.60$) at any pressure. Indeed, in the case of O_2 (see Fig. 6(b)) r^2 is zero at all pressures and thus cannot be displayed within the figure. Strong correlations only begin to be shown when w_{max} is set to 10. PSDs derived from O_2 isotherms do show porosity in the ultramicropore region, thus it may be concluded that the ultramicropores accessible to O_2 are not important for CO_2 uptake, while those ultramicropores accessible to H_2 do contribute to CO_2 uptake. The latter statement can be accounted for by the fact that H_2 has access to pores undetectable by O_2. Similar rationale can be applied to the plot for N_2 (Fig. 6(a)). When w_{max} is increased past 10 Å, r^2 *vs.* P plots become very similar in the case of calculations made

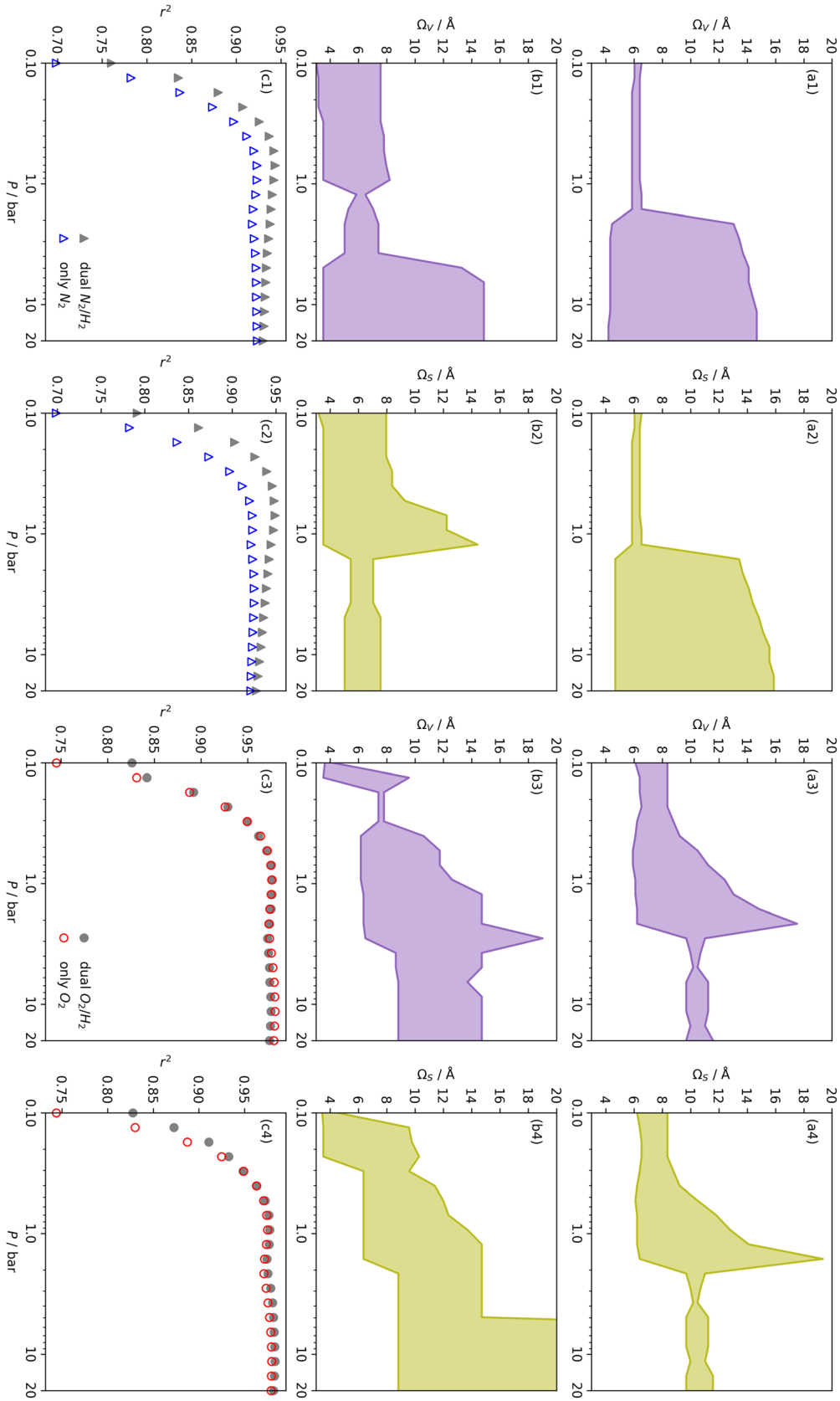

Fig. 7 Comparison of Ω_V (a1, b1, a3, b3) and Ω_S (a2, b2, a4, b4) as determined by N_2 (a1, a2), O_2 (a3, a4) and dual N_2/H_2 (b1, b2) and O_2/H_2 (b3, b4) porosimetry. Row (c) contains comparisons of r^2 with P for the two Ω plots directly above.

using both N_2 and O_2 derived PSDs. This indicates that there is little measurable improvement in CO_2 adsorption (under 2.0 bar) by broadening the PSD past 10 Å, however this may simply be a result of the relatively narrow PSDs present in these samples.

In summary, examination of D_c for DataSet 2 with each of the three porosimetric sorptives shows that low pressure (<2.0 bar) CO_2 uptake is improved by increasing volume in pores below 10 Å. In addition, N_2 is consistently outperformed by O_2 and/or H_2 at measuring porosity appropriate for CO_2 uptake. However, while porosity as determined by O_2 improves CO_2 uptake at pressures above 0.13 bar, H_2 is needed to determine optimum porosity for uptake at ultra-low pressures. It is therefore logical to consider PSDs as determined *via* dual isotherm analysis as a way to extend the range of pressures at which optimum pore size for CO_2 can be accurately determined.

3.2.2 Analysis using PSDs from dual isotherm N_2/H_2 and O_2/H_2 fits. Fitting the 2D-NLDFT heterogeneous surface kernel to H_2 simultaneously with N_2 or O_2 allows the calculation of the range of the PSD in the range 3.0–500 Å. Thus, using these dual-fit PSDs in the calculation of D_c and Ω should allow for consideration of the affinity of all pores in this range for CO_2 in the defined pressure range. Fig. 7 compares Ω_V and Ω_S from single isotherm (N_2 and O_2) fits to those obtained by dual fitting with H_2. In all cases, the Ω *vs.* P plot for the dual fit (Fig. 7(b1–b4)) appears more reasonable than the corresponding plot for single fit (Fig. 7(a1–a4)), especially when P <1.0 bar. In the case of $\Omega_V^{N_2/H_2}$ the improvement over single fit is principally in that the breadth of pore sizes (approx. 3.0–8.0 Å) in $\Omega_V^{N_2/H_2}$ below 1.0 bar is much more realistic than for $\Omega_V^{N_2}$. There is however no broadening within this region with increasing pressure, unlike for $\Omega_S^{N_2/H_2}$ which may be a result of the difference in nature of adsorbate–adsorbent as compared with adsorbate–adsorbate interactions as highlighted in Section 3.1.2. In addition to the relationship between Ω and P being more realistic in terms of both surface area and pore volume, the r^2 is consistently better for both $\Omega_V^{N_2/H_2}$ (c1) and $\Omega_S^{N_2/H_2}$ (c2) than their single-isotherm PSD counterparts. That is to say, that extending the range of accurate, measurable porosity well into the ultramicropore region yields improved certainty in the determination of optimum porosity for CO_2 uptake.

r^2 values for $\Omega_V^{O_2/H_2}$ and $\Omega_S^{O_2/H_2}$ only shows noticeable improvements at pressures below 0.30 bar compared to their single isotherm counterparts (Fig. 7(c3 and c4)). This again indicates the importance of porosity penetrable by H_2 alone in the adsorption of CO_2 at low pressures. For $\Omega_V^{O_2/H_2}$ (Fig. 7(b3)) this corresponds to a significantly smaller range at low pressures, with pores in the range 3.6–4.2 Å being most associated with CO_2 uptake at 0.10 bar, compared to 6.1–8.3 Å for $\Omega_V^{O_2}$ (Fig. 7(a3)). Broadening in $\Omega_V^{O_2/H_2}$ is also briefly apparent as P increases to 0.13 bar, but falls to an unrealistically narrow range again quickly. On the other hand $\Omega_S^{O_2/H_2}$ (Fig. 7(b4)) gives the most physically reasonable result as it broadens consistently with increasing P. Furthermore, we see three distinct values of w_{min} of 3.5, 6.3, and 8.8 Å. The latter two values reflect the results shown in Fig. 1, indicating that the use of dual O_2/H_2 isotherms gives information on the pressures at which the influence of the smallest of ultramicropores on CO_2 uptake is greatest, that is below 0.30 bar.

The utility of dual isotherm porosimetry with H_2 as one of the probes in CO_2 porosity uptake correlations is further emphasised on examination of the dependency of r^2 on P with broadening PSDs (see Fig. 8). In the case of the corresponding plots for single isotherm fits (Fig. 6) H_2 was the only probe molecule that provided strong correlations where w_{max} is 5.0 or 6.0 Å. While dual N_2/H_2 porosimetry (Fig. 8(a)) provides some improvements for these narrow pore width ranges compared to single isotherm N_2 (Fig. 6(a)), the most significant improvements are for O_2/H_2 relative to O_2. Indeed, for all values of w_{max} between 5.0 and 7.0 Å there are reasonable r^2 values (>0.50) (Fig. 8(b)) at some pressure, with w_{max} = 5.0 Å showing the greatest improvement relative to the its single isotherm counterpart. In fact, the plot for 5.0 Å shows improvement even relative to its corresponding plot from single isotherm H_2

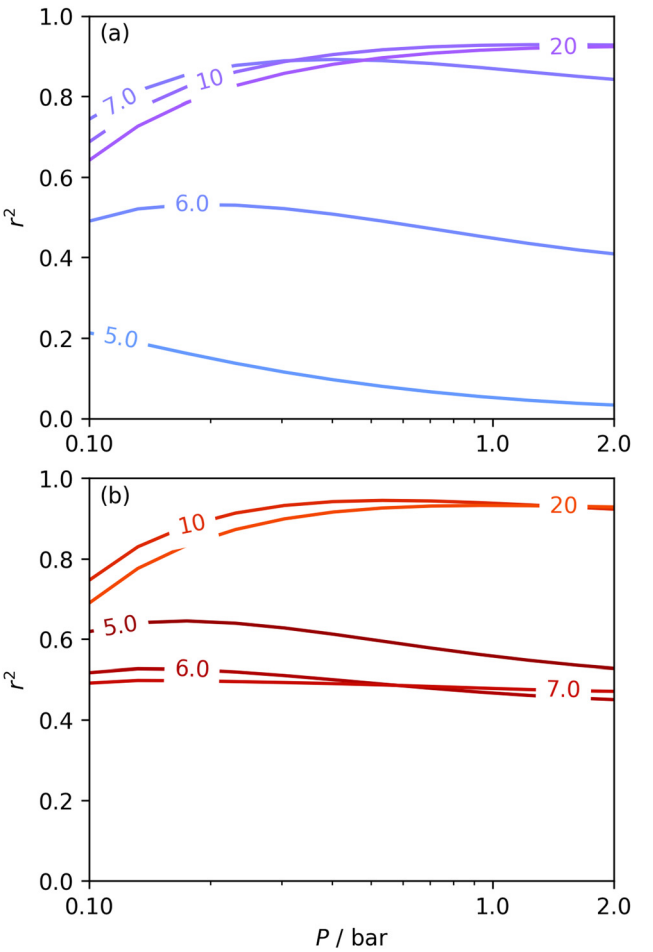

Fig. 8 Comparison of dependence of r^2 on pressure with increasing w_{max} as determined using PSDs from dual N_2/H_2 (a) and O_2/H_2 (b) isotherms.

porosimetry (Fig. 6(c)), as r^2 does not fall below 0.50 at pressures below 5.0 bar. In other words, while H_2 porosimetry shows that pores of width less than 5.0 Å have a reasonable association with CO_2 uptake at 0.10 bar only, combined O_2/H_2 porosimetry shows that this continues to much higher pressures.

It appears therefore that dual O_2/H_2 porosimetry may give a more nuanced and reasonable picture of porosity relevant to CO_2 uptake within samples in DataSet 2 as compared to both dual N_2/H_2 analysis as well as PSDs from single sorptives. In particular, if we compare results from O_2/H_2 analysis to the traditional N_2 analysis it is interesting that the presence of micropores of width <5.0 Å according to the former (Fig. 8(b)) are at least as important as micropores in general according to the latter for CO_2 uptake at very low pressures (see Fig. 8(b) and 6(a), respectively). While more investigation is necessary to determine the precise reasons for the differences in results given by dual isotherm O_2/H_2 and the other methods measurement of the porosity most relevant to CO_2 uptake in highly ultramicroporous carbons, it remains clear that both the certainty of these results from the former and their correspondence with accepted theory of gas adsorption in pores is better.

4 Conclusions

pyPUC shows promise in its ability to thoroughly and definitively elucidate the relationship between porosity within some pore size range, and uptake of a gas at some pressure. We have examined its utility in determining the optimum pore size region in terms of pore volume or surface area (Ω_V or Ω_S) for CO_2 capture in turbostratic carbons at pressures between 0.10 and 40 bar. More than broadly confirming reports by previous experimental and theoretical studies, this work gives a much higher level of precision concerning the relationship between Ω and P. Furthermore, it is possible to approximately predict the increase in CO_2 uptake achieved by increasing porosity within the Ω. Apart from optimum pore sizes ranges, we also find the relationship between pores within arbitrary width ranges on CO_2 uptake.

In addition this method allows facile, comprehensive comparison of such results using different isothermal porosimetric methods for PSD determination. This is particularly relevant to highly ultramicroporous carbons, wherein the utility of N_2 has been called into question. Here, we show that dual isotherm analysis, and in particular O_2/H_2 analysis improves our predictions of CO_2 uptake especially at very low pressures.

The pyPUC method can be easily expanded to be used for calculations related to the uptake of other sorptives, adsorbents, under different conditions, and with other variables (*e.g.* surface chemistry) accounted for. Results from our methods may help improve the design of porous materials for a wide range of adsorption applications.

Author contributions

L. Scott Blankenship: conceptualization, methodology, software, formal analysis, data curation, investigation, writing – original draft, visualization. Nawaf Albeladi: investigation. Thria Alkhaldi: investigation. Asma Madkhali: investigation. Robert Mokaya: validation, resources, writing – review & editing, funding acquisition.

Conflicts of interest

The authors declare that they have no known competing financial interests or personal relationships that could have appeared to influence the work reported in this paper.

Acknowledgements

We are thankful to the EPSRC (Low-Dimensional Materials & Interfaces DTP) for a studentship for L. S. B. In addition, L. S. B. thanks Paul Iacomi for the development of pyGAPS, and assistance with implementation of some of its features in pyPUC as well as to Hassan Akhtar who assisted and advised on some of the code. The use of the University of Nottinghams Augusta HPC service was essential to the completion of this work. We thank the government of the Kingdom of Saudi Arabia for funding PhD studentships for N. A., T. A. and A. M. R. M. thanks the Royal Society for a Royal Society Wolfson Research Merit Award.

Notes and references

1 M. Sevilla and R. Mokaya, *Energy Environ. Sci.*, 2014, **7**, 1250–1280.
2 T. C. Drage, J. M. Blackman, C. Pevida and C. E. Snape, *Energy Fuels*, 2009, **23**, 2790–2796.
3 M. G. Plaza, S. Garcia, F. Rubiera, J. J. Pis and C. Pevida, *Chem. Eng. J.*, 2010, **163**, 41–47.
4 A. Altwala and R. Mokaya, *Energy Environ. Sci.*, 2020, **13**, 2967–2978.
5 S. Biloé, V. Goetz and A. Guillot, *Carbon*, 2002, **40**, 1295–1308.
6 M. Beckner and A. Dailly, *Appl. Energy*, 2016, **162**, 506–514.
7 J. Juan-Juan, J. Marco-Lozar, F. Suárez-García, D. Cazorla-Amorós and A. Linares-Solano, *Carbon*, 2010, **48**, 2906–2909.
8 K.-S. Lin, A. K. Adhikari, K.-C. Chang, C.-L. Chiang and C.-H. Wang, *J. Nanosci. Nanotechnol.*, 2014, **14**, 2700–2708.
9 Q. Zhao, F. Wu, K. Xie, R. Singh, J. Zhao, P. Xiao and P. A. Webley, *Chem. Eng. J.*, 2018, **336**, 659–668.
10 J. Alcaniz-Monge, M. A. de la Casa-Lillo, D. Cazorla-Amorós and A. Linares-Solano, *Carbon*, 1997, **35**, 291–297.
11 D. Lozano-Castello, D. Cazorla-Amoros, A. Linares-Solano and D. F. Quinn, *Carbon*, 2002, **40**, 989–1002.
12 I. Cabria, M. J. López and J. A. Alonso, *Carbon*, 2007, **45**, 2649–2658.
13 V. Presser, J. McDonough, S.-H. Yeon and Y. Gogotsi, *Energy Environ. Sci.*, 2011, **4**, 3059–3066.
14 W. Zhao, V. Fierro, C. Zlotea, E. Aylon, M. Izquierdo, M. Latroche and A. Celzard, *Int. J. Hydrogen Energy*, 2011, **36**, 11746–11751.

15 M. Sevilla, J. B. Parra and A. B. Fuertes, *ACS Appl. Mater. Interfaces*, 2013, **5**, 6360–6368.
16 E. Masika and R. Mokaya, *J. Phys. Chem. C*, 2012, **116**, 25734–25740.
17 Z. Geng, C. Zhang, D. Wang, X. Zhou and M. Cai, *J. Energy Chem.*, 2015, **24**, 1–8.
18 B. Adeniran and R. Mokaya, *Chem. Mater.*, 2016, **28**, 994–1001.
19 Y.-K. Choi and S.-J. Park, *Bull. Korean Chem. Soc.*, 2016, **37**, 830–834.
20 G. Sethia and A. Sayari, *Carbon*, 2016, **99**, 289–294.
21 T. K. Das, S. Banerjee, P. Sharma, V. Sudarsan and P. U. Sastry, *Int. J. Hydrogen Energy*, 2018, **43**, 8385–8394.
22 J. Jagiello, J. Kenvin, A. Celzard and V. Fierro, *Carbon*, 2019, **144**, 206–215.
23 D. Grau-Marin, J. Silvestre-Albero, E. O. Jardim, J. Jagiello, W. R. Betz and L. E. Peña, *Carbon*, 2020, **157**, 495–505.
24 J. Jagiello, J. Kenvin, C. O. Ania, J. B. Parra, A. Celzard and V. Fierro, *Carbon*, 2020, **160**, 164–175.
25 D. H. Everett and J. C. Powl, *J. Chem. Soc., Faraday Trans. 1*, 1976, **72**, 619–636.
26 J. Jagiello and M. Thommes, *International Conference on Carbon for Energy Storage and Environment Protection*, 2005.
27 N. P. Wickramaratne and M. Jaroniec, *J. Mater. Chem. A*, 2013, **1**, 112–116.
28 M. De la Casa-Lillo, F. Lamari-Darkrim, D. Cazorla-Amoros and A. Linares-Solano, *J. Phys. Chem. B*, 2002, **106**, 10930–10934.
29 K. R. Matranga, A. Stella, A. L. Myers and E. D. Glandt, *Sep. Sci. Technol.*, 1992, **27**, 1825–1836.
30 S. Reljic, E. Jardim, C. Cuadrado-Collados, M. Bayona, M. Martinez-Escandell, J. Silvestre-Albero and F. Rodríguez-Reinoso, *CO_2 Adsorption in Activated Carbon Materials,* Springer, 2021, pp. 139–152.
31 N. Texier-Mandoki, J. Dentzer, T. Piquero, S. Saadallah, P. David and C. Vix-Guterl, *Carbon*, 2004, **42**, 2744–2747.
32 Z. Tan and K. E. Gubbins, *J. Phys. Chem.*, 1990, **94**, 6061–6069.
33 C. M. Simon, J. Kim, D. A. Gomez-Gualdron, J. S. Camp, Y. G. Chung, R. L. Martin, R. Mercado, M. W. Deem, D. Gunter and M. Haranczyk, *Energy Environ. Sci.*, 2015, **8**, 1190–1199.
34 L. S. Blankenship, J. Jagiello and R. Mokaya, *Mater. Adv.*, 2022, **3**, 3961–3971.
35 J. Li, B. Michalkiewicz, J. Min, C. Ma, X. Chen, J. Gong, E. Mijowska and T. Tang, *Chem. Eng. J.*, 2019, **360**, 250–259.
36 S.-Y. Lee and S.-J. Park, *J. Colloid Interface Sci.*, 2013, **389**, 230–235.
37 G. Sdanghi, R. L. Canevesi, A. Celzard, M. Thommes and V. Fierro, Characterization of Carbon Materials for Hydrogen Storage and Compression, *C – Journal of Carbon Research*, 2020, **6**(3), 46.
38 S. Hlushak, *Phys. Chem. Chem. Phys.*, 2018, **20**, 872–888.
39 G. Sethia and A. Sayari, *Carbon*, 2015, **93**, 68–80.
40 P. Iacomi and P. L. Llewellyn, *Adsorption*, 2019, **25**, 1533–1542.
41 C. M. Simon, B. Smit and M. Haranczyk, *Comput. Phys. Commun.*, 2016, **200**, 364–380.
42 K. Pearson, *Proc. R. Soc. London*, 1895, **58**, 240–242.
43 J. D. Evans, V. Bon, I. Senkovska and S. Kaskel, *Langmuir*, 2021, **37**, 4222–4226.
44 P. C. Hansen, *SIAM Rev.*, 1992, **34**, 561–580.
45 P. C. Hansen and D. P. OLeary, *SIAM J. Sci. Comput.*, 1993, **14**, 1487–1503.
46 P. Hansen, in *The L-curve and its use in the numerical treatment of inverse problems*, ed. P. Johnston, WIT Press, Southampton, 2001, pp. 119–142.
47 I. Langmuir, *J. Am. Chem. Soc.*, 1916, **38**, 2221–2295.
48 I. Langmuir, *J. Am. Chem. Soc.*, 1918, **40**, 1361–1403.
49 E. A. Guggenheim, *Applications of Statistical Mechanics*, Oxford Clarendon Press, 1966.
50 R. B. Anderson, *J. Am. Chem. Soc.*, 1946, **68**, 686–691.
51 J. H. de Boer, *The Dynamical Character of Adsorption*, Oxford Clarendon Press, 1953, vol. 76.
52 H. Freundlich, *Zeitschrift für Physikalische Chemie*, 1907, **57**, 385–470.
53 B. Bering, M. Dubinin and V. Serpinsky, *J. Colloid Interface Sci.*, 1966, **21**, 378–393.
54 J. Tóth, *J. Colloid Interface Sci.*, 1994, **163**, 299–302.
55 M. E. Casco, M. Martínez-Escandell, J. Silvestre-Albero and F. Rodríguez-Reinoso, *Carbon*, 2014, **67**, 230–235.
56 M. Sevilla, A. S. M. Al-Jumialy, A. B. Fuertes and R. Mokaya, *ACS Appl. Mater. Interfaces*, 2018, **10**, 1623–1633.